

Tiangong-1 Atmospheric Entry Predictions

Introduction

Launched 29 September 2011, *Tiangong-1* served as China's first space station. It hosted visits from an uncrewed *Shenzhou-8* in November 2011, followed by 3-person crews aboard *Shenzhou-9* in June 2012 and *Shenzhou-10* in June 2013. On 21 March 2016, China's Space Engineering Office announced ground communications with *Tiangong-1* had been lost.¹ Figure 1's *Tiangong-1* apsis height history plot corroborates an absence of control capability starting in 2016.² Sudden apsis height increases from propulsive reboost, offsetting intervening intervals of apsis height decay from atmospheric drag, cease after December 2015.

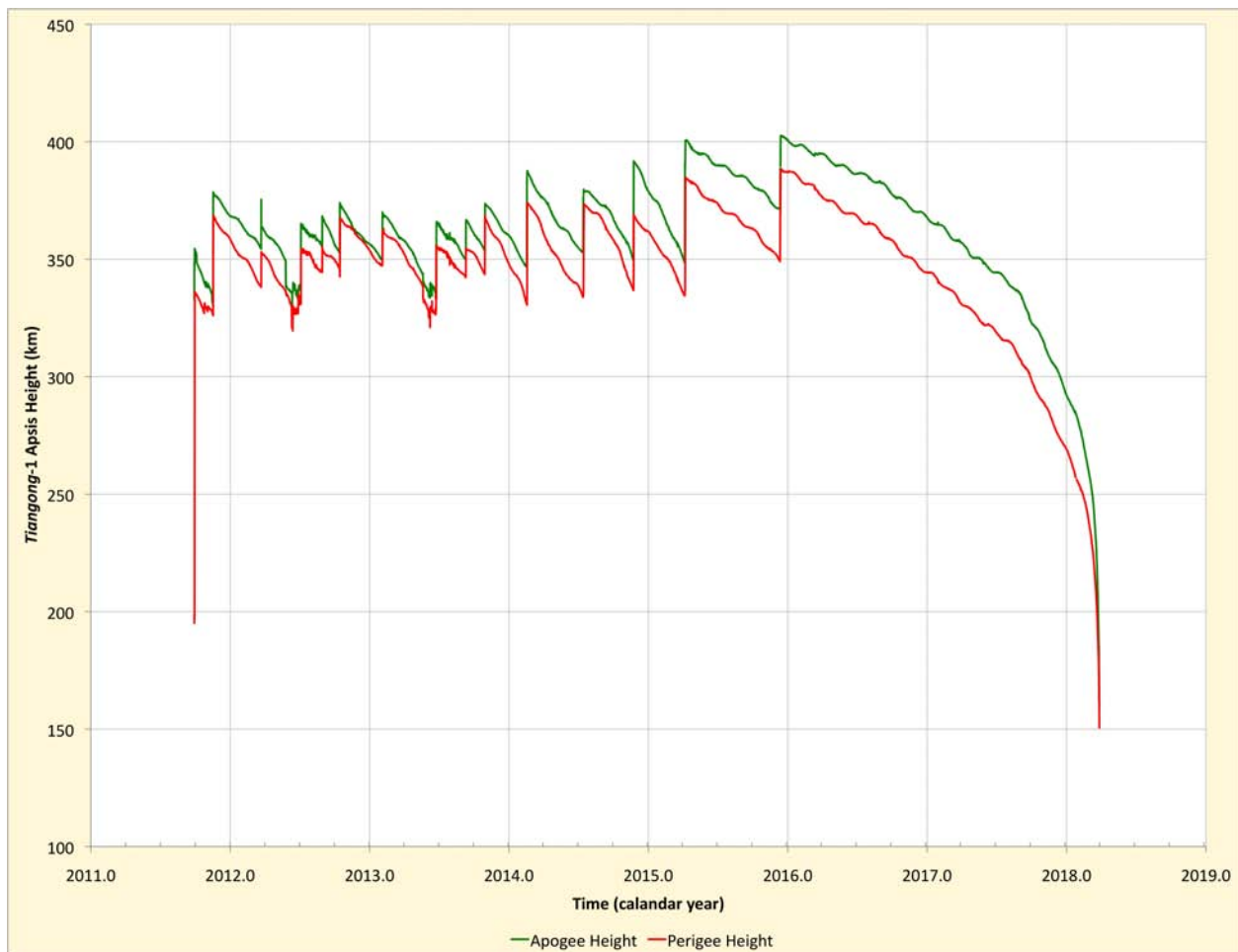


Figure 1. As-flown apogee height (green) and perigee height (red) are plotted as functions of time for *Tiangong-1* from its day of launch until its atmospheric entry and incineration circa 2.0 April 2018 UT.

¹ Reference <https://en.wikipedia.org/wiki/Tiangong-1> (accessed 2 April 2018).

² The source of Figure 1 apsis values and all as-flown *Tiangong-1* trajectory data analyzed in this paper is <https://www.space-track.org/auth/login> (accessed 1 April 2018). In narrative herein, this source is referred to as "Space-Track.org".

Tiangong-1 Atmospheric Entry Predictions

This paper describes methodology applied to predicting *Tiangong-1*'s entry date on a weekly cycle starting in September 2017. Results from this analysis are also documented.

Methodology

Three times are fundamental to *Tiangong-1* entry predictions. The first two times, t_0 and t_1 , define begin and end points, respectively, of a trajectory arc. The i th arc in this analysis is associated with an effective area A_i for *Tiangong-1*'s atmospheric drag acceleration $\ddot{\mathbf{r}}_D$ during that time interval. In all but the final week of *Tiangong-1*'s orbit lifetime, $t_1 - t_0$ is selected from available Space-Track.org two-line element sets (TLEs) to be within a few hours of 7 days. The following parameters are relevant to modeling $\ddot{\mathbf{r}}_D$.

- $C_D \equiv$ *Tiangong-1* coefficient of drag (valued at 2.0 throughout this analysis)
- $m \equiv$ *Tiangong-1* mass = 8506 kg (reference Footnote 1)
- $\rho \equiv$ atmospheric density at *Tiangong-1* geocentric position
- $\mathbf{v} \equiv$ *Tiangong-1* velocity relative to an Earth-fixed coordinate system (note v is the magnitude of \mathbf{v}),

Equation 1 computes $\ddot{\mathbf{r}}_D$, assumed to be the only sensed acceleration when simulating *Tiangong-1* coasted orbit motion.

$$\ddot{\mathbf{r}}_D = -\frac{C_D}{2m} \rho A_i v \mathbf{v} \quad (1)$$

After a value for A_i is developed over the i th t_0 to t_1 arc, it is used with all previous A_i values to refine a running mean value \bar{A} . Coasts are then initiated at t_1 (also termed the "anchor" epoch in this analysis) with \bar{A} replacing A_i in Equation 1. These coasts terminate at the third time, atmospheric entry interface t_{EI} , when *Tiangong-1* simulated geodetic altitude first falls below +121.92 km.

Arguably the most unpredictable parameter in Equation 1 is ρ . This analysis uses a Jacchia-Lineberry dynamic atmosphere [1] to model ρ . In approximating atmospheric heating variations, dynamic atmosphere models typically use empirical measurements expressed as solar flux $F_{10.7}$ and geomagnetic index A_P . For this analysis, the current month's $F_{10.7}$ and A_P values, as last posted before t_1 to https://sail.msfc.nasa.gov/current_solar_report/CurF10.txt (accessed 2 April 2018), are used to develop the corresponding A_i , refine \bar{A} , and perform coasts to t_{EI} .

An attempt to quantify uncertainties in ρ modeling is made by coasting 3 times to t_{EI} for a particular \bar{A} update. Each coast is made with the Jacchia-Lineberry atmosphere configured using distinct $(F_{10.7}, A_P)$ values available for download at sail.msfc. The 95% atmosphere's $(F_{10.7}, A_P)$ values are relatively large and considered to produce 2σ "heavy" ρ , the 50% atmosphere's $(F_{10.7}, A_P)$ values are moderate and considered to produce "mean" or best-guess ρ , and the 5% atmosphere's $(F_{10.7}, A_P)$ values are relatively small and considered to produce 2σ "light" ρ . Thus, as coasts for a given \bar{A} update are made with 95%, 50%, and 5% atmospheres,

Tiangong-1 Atmospheric Entry Predictions

t_{EI} estimates become progressively later to define an entry interface "window" having 2σ confidence.

The value for A_i associated with a particular t_0 to t_1 arc reflects the mean of two effective drag area values obtained in the presence of a 50% atmosphere. The first component of this mean value achieves a near-null along-track position deviation ΔV from *Tiangong-1*'s TLE at t_1 , while the mean value's second component achieves a near-null semi-major axis deviation Δa from the t_1 TLE. Example iterations producing A_i for a specific *Tiangong-1* arc appear in Table 1.³

Table 1. Iterations in \ddot{r}_D reference area A with a 50% atmosphere leading to near-null along-track position deviation ΔV (red) and near-null semi-major axis deviation Δa (green) are reproduced for the coasting arc from $t_0 = 19$ February 2018 @ 10:39 UT to $t_1 = 26$ February 2018 @ 09:45 UT. The final value for A (blue) is the mean of those achieving the two near-null conditions and becomes A_{24} in this analysis. The ΔV and Δa associated with A_{24} in this table are termed the iteration's residuals.

A (m ²)	ΔV (km)	Δa (km)
28.138	+344.862	-0.947645
25.138	-6.236	-0.240152
25.192	+0.046	-0.252775
24.111	-125.471	-0.000690
24.108	-125.819	+0.000008
24.650	-62.958	-0.126195

The WeavEncke predictor [2] numerically integrates all simulated *Tiangong-1* trajectory coasts. In addition to \ddot{r}_D , WeavEncke simulates Earth gravity from the GEM10 model truncated to 7th degree and order. Also simulated in *Tiangong-1* coasts is gravity from the Sun and Moon modeled as point sources.

Results

Figure 2 plots A_i and \bar{A} as functions of the associated t_1 UT. With little statistic weight early in this analysis, \bar{A} tends to be relatively "noisy" and subject to change. As the number of A_i values comprising \bar{A} 's running average increases, however, \bar{A} statistic inertia grows. This imbedded history and insensitivity to short-term changes makes \bar{A} particularly well-suited for simulated coasts to t_{EI} over many weeks or months. Because A_i values are localized in time with respect to \bar{A} , they must compensate for transient atmospheric heating effects from solar flares and geomagnetic storms affecting the real world ρ . Particularly at times late in this analysis, A_i values would become influenced by changes in *Tiangong-1*'s rotational state as it begins to tumble at higher rates in response to aerodynamic torques. Both A_i and m are subject to change if appendages are lost just before atmospheric entry.

³ As is evident from Table 1 values, ΔV is signed such that a positive value is down-track with respect to the TLE at t_1 . To correct $\Delta V > 0$ toward a null deviation requires A be reduced in the next iteration. Similarly, Δa is signed such that a positive value has a larger semi-major axis (or, equivalently, mean geocentric orbit height) with respect to the TLE at t_1 . To correct $\Delta a > 0$ toward a null deviation requires A be increased in the next iteration.

Tiangong-1 Atmospheric Entry Predictions



Figure 2. Values for A_i (green) and \bar{A} (orange) are plotted as functions of anchor date t_1 as this analysis is conducted during the final half year of *Tiangong-1*'s orbit lifetime. Although the two functions must have equal values initially by definition, there is no guarantee this condition will be approached to any great precision subsequently. But such appears to be the case for the final A_{31} value with $t_1 = 1$ April 2018 @ 11:45 UT.

If Equation 1 were to perfectly model real world \ddot{r}_D , each A_i would be associated with $\Delta V = \Delta a = 0$ residuals. Figure 3's plot of these residuals as functions of t_1 helps quantify the degree to which Equation 1 idealizes reality when simulating *Tiangong-1* orbit coasts. As intuition would suggest, residuals are greatest in magnitude as *Tiangong-1* nears entry. The Figure 3 residuals spike in mid-March 2018 cannot be attributed to ρ modeling errors alone. It is likely *Tiangong-1* was in a chaotic rotational state induced by aerodynamic torques at this time. Another possible cause of this spike in residuals would be venting from pressurized onboard systems. A post-entry check of the Space-Track.org satellite catalog (SATCAT) indicates no unclassified debris associated with *Tiangong-1* had been detected during the space station's orbit lifetime.

Tiangong-1 Atmospheric Entry Predictions

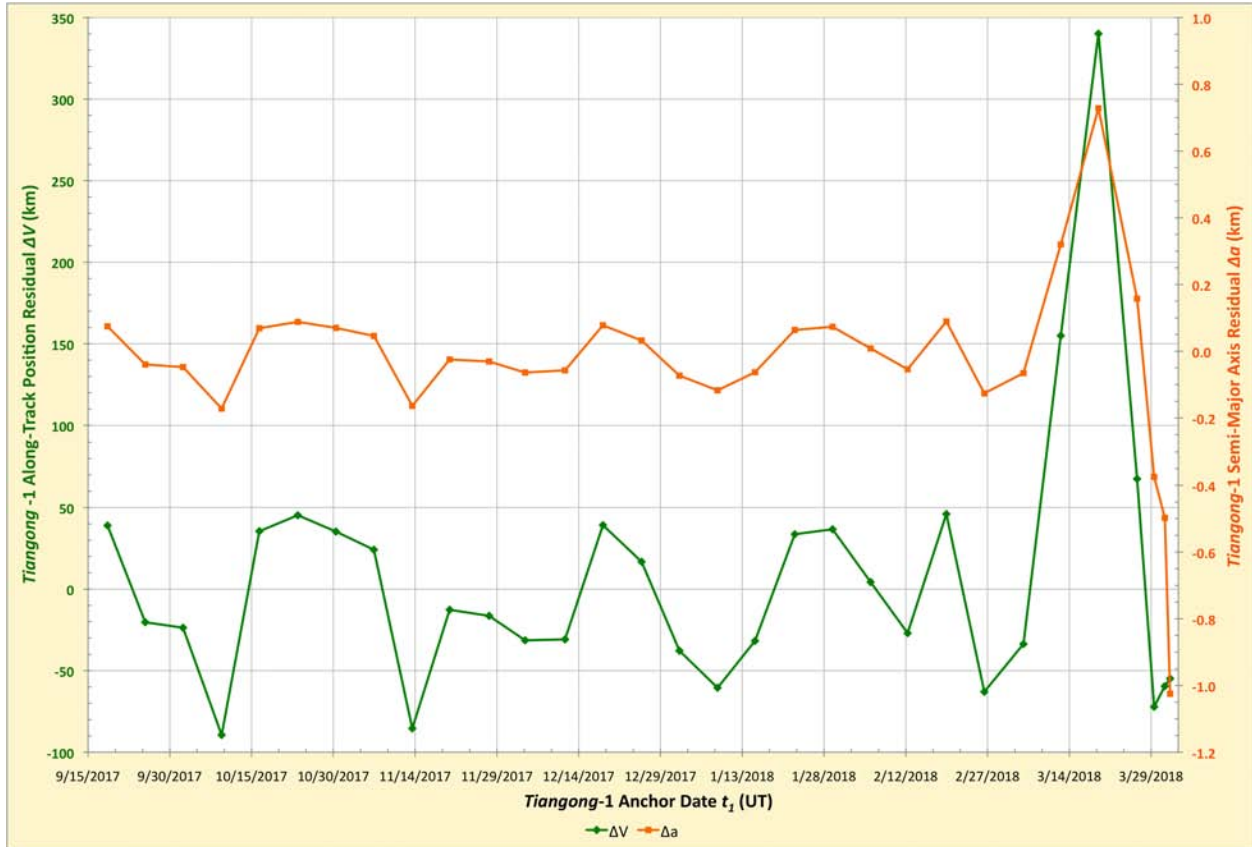


Figure 3. Residuals associated with A_i iterations (reference Table 1's example) are plotted as functions of t_1 . The along-track position residual ΔV function and scale are colored green, while the semi-major axis residual Δa function and scale are colored orange. Note the null condition for ΔV is nearly 3 horizontal grid lines below the null condition for Δa .

Figures 4 and 5 are plots of t_{EI} as a function of the associated anchor epoch t_1 for 95%, 50%, and 5% atmospheres. Entry predictions posted at Space-Track.org are included in these plots. In doing so, the associated message publication time is equated with t_1 . In both figures, note how entry interface windows defined by the 95%, 50%, and 5% plots are enveloped within Space-Track.org markers with only one exception (namely the Figure 5 marker lying very close to the 50% plot). Once the 5% curve peaks with the latest t_{EI} for $t_1 = 19.4$ February 2018 in Figure 4, all subsequent entry interface windows converge in a consistent manner. That is, each window is contained within its predecessors.

Tiangong-1 Atmospheric Entry Predictions

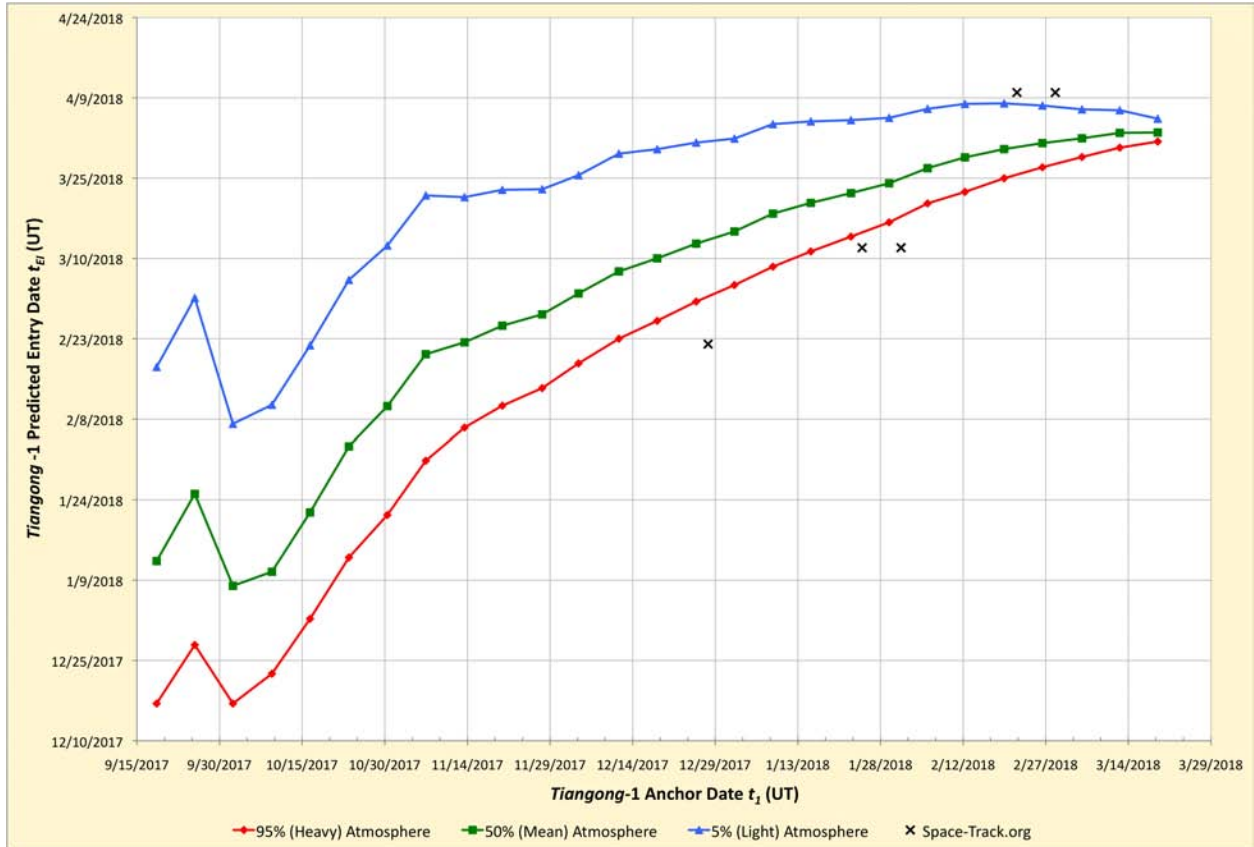


Figure 4. For 95% heavy (red), 50% mean (green), and 5% light (blue) atmospheres, predicted t_{EI} is plotted as a function of anchor epoch with t_I extending from 18.6 September 2017 UT to 19.3 March 2018 UT. Contemporaneous predictions posted at Space-Track.org are plotted with black "X" markers.

Tiangong-1 Atmospheric Entry Predictions

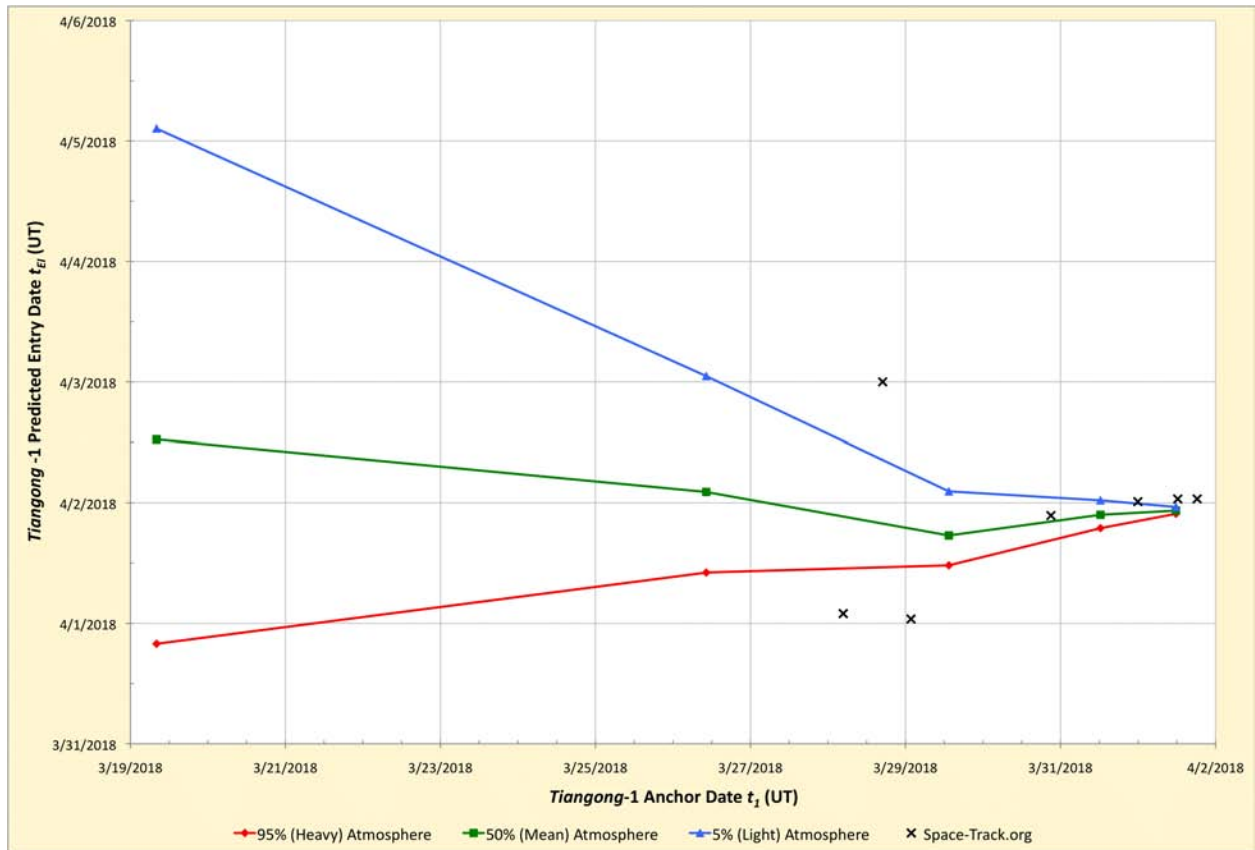


Figure 5. For 95% heavy (red), 50% mean (green), and 5% light (blue) atmospheres, predicted t_{EI} is plotted as a function of anchor epoch with t_I extending from 19.3 March 2018 UT to 1.5 April 2018 UT. Contemporaneous predictions posted at Space-Track.org are plotted with black "X" markers.

The Figure 6 ground track plot reflects a 50% coast from the final $t_I = 1$ April 2018 @ 11:45 UT in Figure 5 to 22:00 UT. To inhibit premature termination of the ground track at the corresponding 50% $t_{EI} = 1$ April 2018 @ 22:28 UT, \ddot{r}_D is set to zero after 22:00 UT. This permits a reasonably accurate illustration of *Tiangong-1* position at the time Space-Track.org declares actual atmospheric entry occurred: 2 April 2018 @ 00:00 UT.

Tiangong-1 Atmospheric Entry Predictions

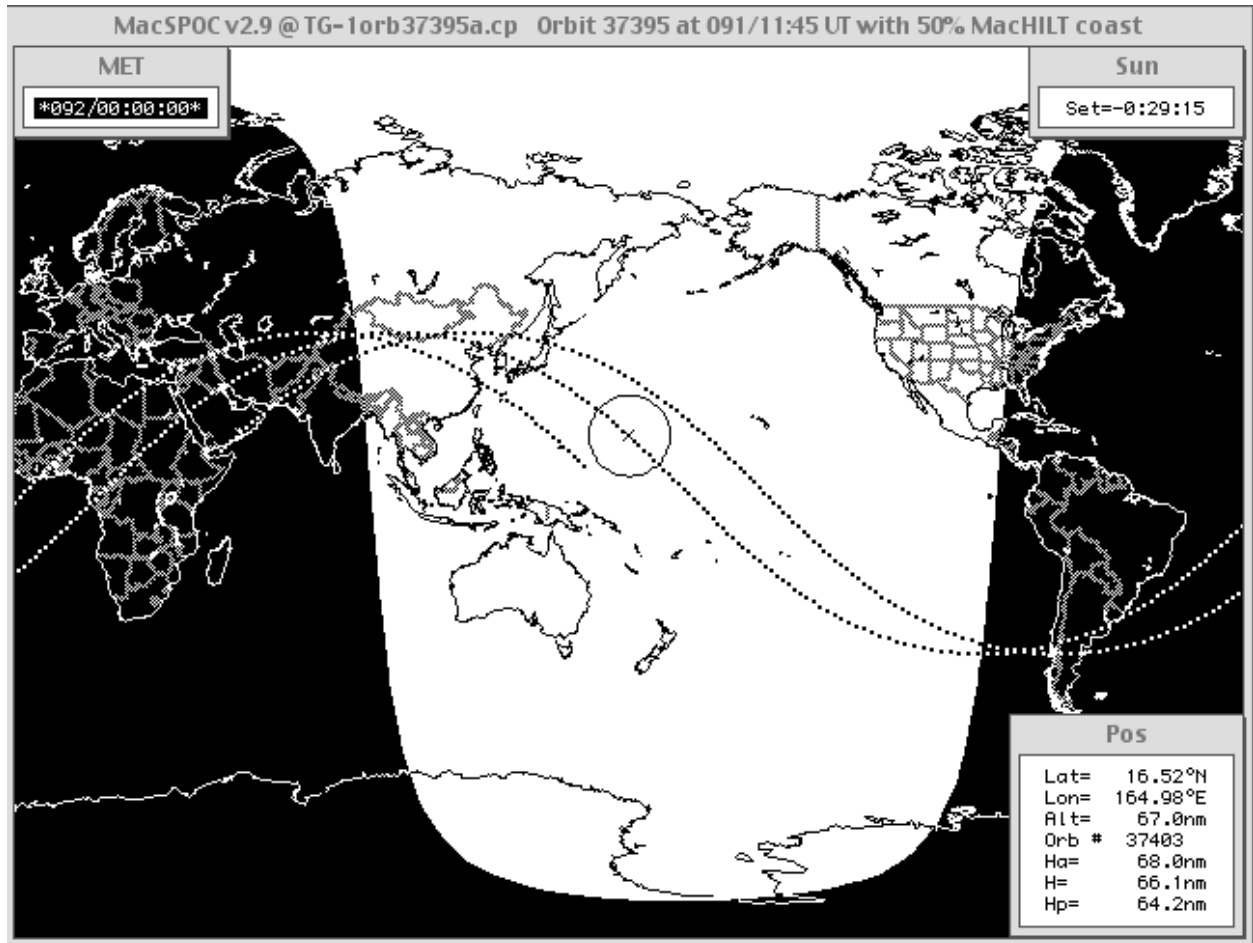


Figure 6. The *Tiangong-1* ground track is mapped around the time of its atmospheric entry as a series of 2-pixel-square markers at 30-s intervals. Simulated current time in DOY/HH:MM:SS UT is displayed in the MET window and corresponds to 2.0 April 2018 UT, when Space-Track.org declares entry occurred. Coasted *Tiangong-1* position at this time coincides with the small "X" west of Hawaii⁴ and is circumscribed by points mapping *Tiangong-1*'s simulated current Earth horizon. Reverse-field regions on the map correspond to Earth's nightside on April 2.0 UT.

Concluding Remarks

Analysis techniques documented in this paper have produced results satisfyingly consistent with *Tiangong-1* atmospheric entry predictions appearing on Space-Track.org and in news media reports during the final months of this space station's orbit lifetime. The last entry prediction using these techniques, based on an anchor epoch of 1 April 2018 @ 11:45 UT, is about an orbit earlier than the 2.0 April UT entry time declared by Space-Track.org as actual. It should be noted the last TLE posted by Space-Track.org has an April 1 epoch of 16:07 UT, so there

⁴ To reiterate remarks in the accompanying narrative, coasted motion after the start of Figure 6's ground track (off the coast of Yemen at 22:01 UT) is with zero drag acceleration because the associated t_{EI} would otherwise be 1 April @ 22:28 UT, about an orbit earlier than the simulated current time at which Space-Track.org declares entry occurred.

Tiangong-1 Atmospheric Entry Predictions

appears to be no publicly available empirical data with which to infer a *Tiangong-1* entry time to much better precision than about an orbit or 1.5 hours.

Given controlled satellite disposal techniques via destructive atmospheric entry routinely target the South Pacific Ocean (*Mir* and *Progress* being good examples), it would be hard to achieve a better outcome for *Tiangong-1* than is indicated in Figure 6. This lends credence to speculation there may have been a non-propulsive means of controlling *Tiangong-1*'s entry trajectory to some limited extent. Speculation along these lines is further supported by a Reuters report published early in 2018.⁵ Do the Chinese have something to teach us about safe satellite disposal via destructive atmospheric entry?

References

- [1] Mueller, A. C., "Jacchia-Lineberry Upper Atmosphere Density Model", Internal Note 82-FM-52, NASA JSC-18507, October 1982.⁶

- [2] Adamo, D. R., "A Precision Orbit Predictor Optimized for Complex Trajectory Operations", AAS 03-665, *Volume 116 of the Advances in the Astronautical Sciences*, Univelt, San Diego, pp. 2567-2586, 2003.

⁵ Reference <https://www.reuters.com/article/us-china-space/chinas-tiangong-1-space-lab-is-not-out-of-control-top-chinese-engineer-idUSKBN1EX09H> (accessed 5 April 2018)

⁶ This document may be downloaded at <https://ntrs.nasa.gov/archive/nasa/casi.ntrs.nasa.gov/19830012203.pdf> (accessed 2 April 2018).